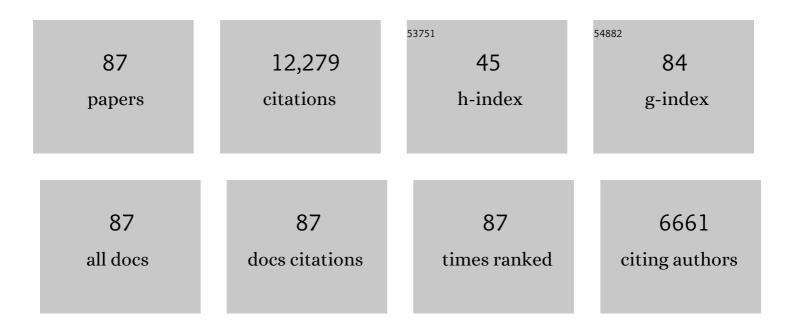
## C Cem Tasan

List of Publications by Year in descending order

Source: https://exaly.com/author-pdf/4127990/publications.pdf Version: 2024-02-01



#	Article	IF	CITATIONS
1	In-situ investigation of plasticity in a Ti-Al-V-Fe (α+β) alloy: Slip mechanisms, strain localization, and partitioning. International Journal of Plasticity, 2022, 148, 103131.	4.1	48
2	Towards physical insights on microstructural damage nucleation from data analytics. Computational Materials Science, 2022, 202, 110627.	1.4	1
3	In-situ scanning electron microscope thermal desorption spectroscopy (SEM-TDS) analysis of thermally-induced titanium hydride decomposition and reformation. Acta Materialia, 2022, 226, 117562.	3.8	4
4	Chemo-mechanical effects on the cutting-induced mixed-mode II-III fracture of martensitic stainless steels: An in-situ investigation. Acta Materialia, 2022, 231, 117803.	3.8	2
5	Sustainability through alloy design: Challenges and opportunities. Progress in Materials Science, 2021, 117, 100722.	16.0	58
6	Enhancing damage-resistance in low carbon martensitic steels upon dual-pass laser treatment. Scripta Materialia, 2021, 192, 13-18.	2.6	12
7	Slip-twinning interdependent activation across phase boundaries: An in-situ investigation of a Ti-Al-V-Fe (α+β) alloy. Acta Materialia, 2021, 206, 116520.	3.8	41
8	Carbon redistribution in quenched and tempered lath martensite. Acta Materialia, 2021, 205, 116521.	3.8	60
9	Hydride formation in Ti6Al4V: An in situ synchrotron X-ray diffraction study. Scripta Materialia, 2021, 193, 12-16.	2.6	14
10	In-situ investigation of strain partitioning and microstructural strain path development up to and beyond necking. Acta Materialia, 2021, 215, 117023.	3.8	19
11	Element-resolved local lattice distortion in complex concentrated alloys: An observable signature of electronic effects. Acta Materialia, 2021, 216, 117135.	3.8	22
12	Roughening improves hydrogen embrittlement resistance of Ti-6Al-4V. Acta Materialia, 2021, 220, 117304.	3.8	23
13	Composition-dependent slip planarity in mechanically-stable face centered cubic complex concentrated alloys and its mechanical effects. Acta Materialia, 2021, 220, 117314.	3.8	24
14	Influence of co-existing medium Mn and dual phase steel microstructures on ductility and Lüders band formation. Acta Materialia, 2021, 221, 117418.	3.8	20
15	Tuning mechanical metastability in FeMnCo medium entropy alloys and a peek into deformable hexagonal close-packed martensite. Applied Physics Letters, 2021, 119, 261905.	1.5	3
16	Tracking Microstructure Evolution in Complex Biaxial Strain Paths: A Bulge Test Methodology for the Scanning Electron Microscope. Experimental Mechanics, 2020, 60, 35-50.	1.1	2
17	Laser-induced toughening inhibits cut-edge failure in multi-phase steel. Scripta Materialia, 2020, 177, 79-85.	2.6	6
18	High entropy alloys: A focused review of mechanical properties and deformation mechanisms. Acta Materialia, 2020, 188, 435-474.	3.8	921

#	Article	IF	CITATIONS
19	Deformation faulting in a metastable CoCrNiW complex concentrated alloy: A case of negative intrinsic stacking fault energy?. Acta Materialia, 2020, 200, 992-1007.	3.8	45
20	Strong Macroscale Supercrystalline Structures by 3D Printing Combined with Selfâ€Assembly of Ceramic Functionalized Nanoparticles. Advanced Engineering Materials, 2020, 22, 2070028.	1.6	2
21	Design of a V–Ti–Ni alloy with superelastic nano-precipitates. Acta Materialia, 2020, 196, 710-722.	3.8	5
22	Damage in metal forming. CIRP Annals - Manufacturing Technology, 2020, 69, 600-623.	1.7	64
23	How hair deforms steel. Science, 2020, 369, 689-694.	6.0	23
24	Natural-mixing guided design of refractory high-entropy alloys with as-cast tensile ductility. Nature Materials, 2020, 19, 1175-1181.	13.3	209
25	Strong Macroscale Supercrystalline Structures by 3D Printing Combined with Selfâ€Assembly of Ceramic Functionalized Nanoparticles. Advanced Engineering Materials, 2020, 22, 2000352.	1.6	19
26	Effects of Defect Development During Displacive Austenite Reversion on Strain Hardening and Formability. Metallurgical and Materials Transactions A: Physical Metallurgy and Materials Science, 2020, 51, 3832-3842.	1.1	0
27	Origin of micrometer-scale dislocation motion during hydrogen desorption. Science Advances, 2020, 6, eaaz1187.	4.7	29
28	Hydrogenation-induced lattice expansion and its effects on hydrogen diffusion and damage in Ti–6Al–4V. Acta Materialia, 2020, 188, 686-696.	3.8	42
29	Manganese micro-segregation governed austenite re-reversion and its mechanical effects. Scripta Materialia, 2020, 179, 75-79.	2.6	16
30	Plastic strain-induced sequential martensitic transformation. Scripta Materialia, 2020, 185, 36-41.	2.6	22
31	Interstitial-Free Bake Hardening Realized by Epsilon Martensite Reverse Transformation. Metallurgical and Materials Transactions A: Physical Metallurgy and Materials Science, 2019, 50, 3985-3991.	1.1	9
32	Strategies for improving the sustainability of structural metals. Nature, 2019, 575, 64-74.	13.7	301
33	Avoiding FIB damage using the "umbrella―method. Microscopy and Microanalysis, 2019, 25, 850-851.	0.2	0
34	Diffraction-based misorientation mapping: A continuum mechanics description. Journal of the Mechanics and Physics of Solids, 2019, 133, 103709.	2.3	57
35	Boundary micro-cracking in metastable Fe45Mn35Co10Cr10 high-entropy alloys. Acta Materialia, 2019, 168, 76-86.	3.8	72
36	Microstructural and micro-mechanical characterization during hydrogen charging: An in situ scanning electron microscopy study. International Journal of Hydrogen Energy, 2019, 44, 6333-6343.	3.8	42

#	Article	IF	CITATIONS
37	Engineering atomic-level complexity in high-entropy and complex concentrated alloys. Nature Communications, 2019, 10, 2090.	5.8	182
38	Microstructural damage sensitivity prediction using spatial statistics. Scientific Reports, 2019, 9, 2774.	1.6	7
39	Phase Stability Effects on Hydrogen Embrittlement Resistance in Martensite–Reverted Austenite Steels. Metallurgical and Materials Transactions A: Physical Metallurgy and Materials Science, 2019, 50, 29-34.	1.1	12
40	Fatigue Resistance of Laminated and Non-laminated TRIP-maraging Steels: Crack Roughness vs Tensile Strength. Metallurgical and Materials Transactions A: Physical Metallurgy and Materials Science, 2019, 50, 1142-1145.	1.1	8
41	Strain-programmable fiber-based artificial muscle. Science, 2019, 365, 145-150.	6.0	298
42	Experimental–numerical study on strain and stress partitioning in bainitic steels with martensite–austenite constituents. International Journal of Plasticity, 2018, 104, 39-53.	4.1	48
43	Microstructural mechanisms of fatigue crack non-propagation in TRIP-maraging steels. International Journal of Fatigue, 2018, 113, 126-136.	2.8	23
44	Preventing damage and redeposition during focused ion beam milling: The "umbrella―method. Ultramicroscopy, 2018, 186, 35-41.	0.8	30
45	Multiresolution mechanical characterization of hierarchical materials: Spherical nanoindentation on martensitic Fe-Ni-C steels. Acta Materialia, 2018, 153, 257-269.	3.8	26
46	Comparative study of hydrogen embrittlement in stable and metastable high-entropy alloys. Scripta Materialia, 2018, 150, 74-77.	2.6	84
47	Metastability in high-entropy alloys: A review. Journal of Materials Research, 2018, 33, 2924-2937.	1.2	85
48	Interstitial atoms enable joint twinning and transformation induced plasticity in strong and ductile high-entropy alloys. Scientific Reports, 2017, 7, 40704.	1.6	279
49	Complexion-mediated martensitic phase transformation in Titanium. Nature Communications, 2017, 8, 14210.	5.8	71
50	Bone-like crack resistance in hierarchical metastable nanolaminate steels. Science, 2017, 355, 1055-1057.	6.0	297
51	Recent progress in microstructural hydrogen mapping in steels: Quantification, kinetic analysis, and multi-scale characterisation. Materials Science and Technology, 2017, 33, 1481-1496.	0.8	125
52	Martensite size effects on damage in quenching and partitioning steels. Scripta Materialia, 2017, 138, 1-5.	2.6	55
53	Effects of lamella size and connectivity on fatigue crack resistance of TRIP-maraging steel. International Journal of Fatigue, 2017, 100, 176-186.	2.8	19
54	A TRIP-assisted dual-phase high-entropy alloy: Grain size and phase fraction effects on deformation behavior. Acta Materialia, 2017, 131, 323-335.	3.8	474

#	Article	IF	CITATIONS
55	Designing duplex, ultrafine-grained Fe-Mn-Al-C steels by tuning phase transformation and recrystallization kinetics. Acta Materialia, 2017, 141, 374-387.	3.8	77
56	Improved Atom Probe Methodology for Studying Carbon Redistribution in Low-Carbon High-Ms Lath Martensitic Steels. Microscopy and Microanalysis, 2017, 23, 706-707.	0.2	4
57	Partial recrystallization of gum metal to achieve enhanced strength and ductility. Acta Materialia, 2017, 135, 400-410.	3.8	38
58	In situ observations of silver-decoration evolution under hydrogen permeation: Effects of grain boundary misorientation on hydrogen flux in pure iron. Scripta Materialia, 2017, 129, 48-51.	2.6	66
59	Metastable high-entropy dual-phase alloys overcome the strength–ductility trade-off. Nature, 2016, 534, 227-230.	13.7	2,612
60	Multiple mechanisms of lath martensite plasticity. Acta Materialia, 2016, 121, 202-214.	3.8	190
61	Spectral TRIP enables ductile 1.1ÂGPa martensite. Acta Materialia, 2016, 111, 262-272.	3.8	141
62	Multi-probe microstructure tracking during heat treatment without an in-situ setup: Case studies on martensitic steel, dual phase steel and β-Ti alloy. Materials Characterization, 2016, 111, 137-146.	1.9	17
63	From Highâ€Entropy Alloys to Highâ€Entropy Steels. Steel Research International, 2015, 86, 1127-1138.	1.0	158
64	3D structural and atomic-scale analysis of lath martensite: Effect of the transformation sequence. Acta Materialia, 2015, 95, 366-377.	3.8	191
65	Damage resistance in gum metal through cold work-induced microstructural heterogeneity. Journal of Materials Science, 2015, 50, 5694-5708.	1.7	10
66	High resolution in situ mapping of microstrain and microstructure evolution reveals damage resistance criteria in dual phase steels. Acta Materialia, 2015, 96, 399-409.	3.8	182
67	Origin of shear induced β to ω transition in Ti–Nb-based alloys. Acta Materialia, 2015, 92, 55-63.	3.8	129
68	Design of a twinning-induced plasticity high entropy alloy. Acta Materialia, 2015, 94, 124-133.	3.8	618
69	An Overview of Dual-Phase Steels: Advances in Microstructure-Oriented Processing and Micromechanically Guided Design. Annual Review of Materials Research, 2015, 45, 391-431.	4.3	469
70	Retardation of plastic instability via damage-enabled microstrain delocalization. Journal of Materials Science, 2015, 50, 6882-6897.	1.7	45
71	Non-equiatomic high entropy alloys: Approach towards rapid alloy screening and property-oriented design. Materials Science & Engineering A: Structural Materials: Properties, Microstructure and Processing, 2015, 648, 183-192.	2.6	166
72	Deformation mechanism of ω-enriched Ti–Nb-based gum metal: Dislocation channeling and deformation induced ω–β transformation. Acta Materialia, 2015, 100, 290-300.	3.8	138

#	Article	IF	CITATIONS
73	Enhancing Hydrogen Embrittlement Resistance of Lath Martensite by Introducing Nano-Films of Interlath Austenite. Metallurgical and Materials Transactions A: Physical Metallurgy and Materials Science, 2015, 46, 3797-3802.	1.1	77
74	Nanolaminate transformation-induced plasticity–twinning-induced plasticity steel with dynamic strain partitioning and enhanced damage resistance. Acta Materialia, 2015, 85, 216-228.	3.8	207
75	Composition Dependence of Phase Stability, Deformation Mechanisms, and Mechanical Properties of the CoCrFeMnNi High-Entropy Alloy System. Jom, 2014, 66, 1993-2001.	0.9	135
76	Hydrogen-assisted decohesion and localized plasticity in dual-phase steel. Acta Materialia, 2014, 70, 174-187.	3.8	366
77	Smaller is less stable: Size effects on twinning vs. transformation of reverted austenite in TRIP-maraging steels. Acta Materialia, 2014, 79, 268-281.	3.8	225
78	Integrated experimental–simulation analysis of stress and strain partitioning in multiphase alloys. Acta Materialia, 2014, 81, 386-400.	3.8	285
79	Strain localization and damage in dual phase steels investigated by coupled in-situ deformation experiments and crystal plasticity simulations. International Journal of Plasticity, 2014, 63, 198-210.	4.1	412
80	A novel, single phase, non-equiatomic FeMnNiCoCr high-entropy alloy with exceptional phase stability and tensile ductility. Scripta Materialia, 2014, 72-73, 5-8.	2.6	534
81	On dislocation involvement in Ti–Nb gum metal plasticity. Scripta Materialia, 2013, 68, 805-808.	2.6	39
82	Identification of the continuum damage parameter: An experimental challenge in modeling damage evolution. Acta Materialia, 2012, 60, 3581-3589.	3.8	77
83	Microstructural banding effects clarified through micrographic digital image correlation. Scripta Materialia, 2010, 62, 835-838.	2.6	158
84	Indentation-based damage quantification revisited. Scripta Materialia, 2010, 63, 316-319.	2.6	24
85	Experimental analysis of strain path dependent ductile damage mechanics and forming limits. Mechanics of Materials, 2009, 41, 1264-1276.	1.7	94
86	A critical assessment of indentation-based ductile damage quantification. Acta Materialia, 2009, 57, 4957-4966.	3.8	32
87	Hydrogen-Induced Martensitic Transformation and Twinning in Fe45Mn35Cr10Co10. Metallurgical and Materials Transactions A: Physical Metallurgy and Materials Science, 0, , 1.	1.1	3